Journal of Fluids and Structures (2000) **14,** 511–528
doi:10.1006/jfls.1999.0284, available online at http://www.idealibrary.com on IDEAL®

THE SELF-INDUCED FREE-SURFACE "SWELL FLAPPING" CAUSED BY THE INTERACTION AMONG A JET, A FREE SURFACE AND A STRUCTURE

S. Someya, K. Okamoto and H. Madarame

Nuclear Engineering Research Laboratory, The University of Tokyo
Tokai-mura, Ibaraki, 319-1106, Japan

(Received 14 April 1999; and in final form 26 November 1999)

A new type of self-induced free-surface oscillation (swell flapping) was discovered in a system with a jet, a free surface and a structure. An upward round jet was injected into a cylindrical tank from the bottom centre. The jet impinged on the bottom of an upper-inner-structure (UIS) in a LMFBR nuclear reactor, which was set just beneath the free surface and above the jet inlet channel. The jet was separated at the edge of the UIS. In the cylindrical tank system, the effects of the geometric parameters on the occurrence and period of the swell flapping were investigated. The swell height during the oscillation was thought to be important; therefore, the experiments were made with a rectangular tank system in order to measure the swell height. Swell flapping was also observed in the rectangular tank. At a certain jet inlet velocity and UIS depth, the separated jet oscillated, forming a swell of the free surface around the UIS. The maximum swell height from the bottom edge of the UIS increases proportionately with the jet inlet velocity, independently of the UIS depth. The period of oscillation increases with increasing swell height and velocity. The period of oscillation was divided into a swell rising component and a swell breaking component. The time required for swell rising depended on the jet inlet velocity, while that required for swell breaking corresponded to the wave propagation period.
© 2000 Academic Press

1. INTRODUCTION

The liquid metal fast breeder reactor (LMFBR) has a free surface in a pool of sodium and an upper-inner-structure (UIS) above the core in the reactor vessel (Inagaki et al. 1987). In the FBR, the relatively high-speed circulating flow may interact with the free surface or the UIS. If the free surface or the circulating flow oscillates, it may induce high thermal stresses in the vessel wall due to the high thermal conductivity of sodium (Hara 1990). Also in terms of operating mass flow-rate and reactivity, it is important to investigate the flow fluctuation.

The self-induced oscillations of a jet have already been studied (Fukaya *et al.* 1995). For example, "Jet-Flutter" (Madarame *et al.* 1993) was the lateral oscillation of the jet synchronizing with the surface swell fluctuation. "Jet-Flutter" was observed when a jet injected into a tank and impinged on a free surface, generating a swell.

However, few papers discussed the interaction in a system having a jet, a free surface and a structure. It is important to discuss the interaction in such a system in order to evaluate the performance of the FBR.

In this study, experiments were carried out to investigate the interaction among an upward jet, a free surface and an UIS. A new kind of self-induced surface oscillation was observed in these experiments. The characteristics of the oscillation were experimentally evaluated.

0889–9746/00/050511 + 18 $35.00/0 © 2000 Academic Press

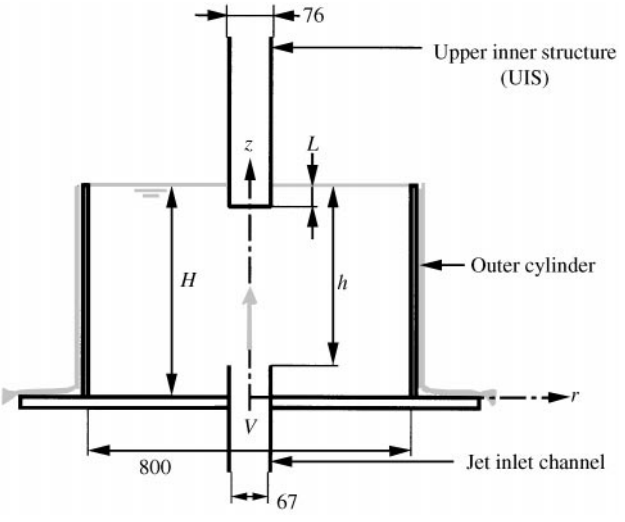

Figure 1. Cross-sectional view of the cylindrical test tank; dimensions in mm.

TABLE 1

Geometric parameters

Group	*L*	*h*	*H*
Standard	40	300	400
I	10–120	300	400
II	40	200–400	400
III	40	300	300–500

2. EXPERIMENTS IN A CYLINDRICAL TANK SYSTEM

2.1. EXPERIMENTAL APPARATUS

At first, experiments were carried out with a cylindrical tank system. A cross-sectional view of the axisymmetric experimental apparatus is shown schematically in Figure 1. The experimental apparatus was composed of a cylindrical tank, a jet inlet channel and the UIS, which had a common vertical axis of symmetry. The cylindrical tank was made of transparent acrylic resin, 5 mm thick, with an 800 mm inner diameter. All components of the test-section were firmly fixed, so that they could not vibrate.

The water level of the test tank was controlled by the height of the cylindrical tank, which played the role of a weir. Since the difference between the actual water level and the height of the cylindrical tank was small, the water level, H, was defined as the height of the cylindrical tank in this apparatus. The jet inlet channel, 67 mm in inner diameter, could be extended into the tank from the bottom centre. The distance from inlet to surface, h, was defined as the water depth of the jet inlet channel, which was varied by changing the protruding length of the jet inlet channel. The UIS, 76 mm in outer diameter, was submerged in the water just above the jet inlet channel. The UIS depth, L, was defined as the distance between the water surface and the bottom of the UIS, as shown in Figure 1.

In the experiment, three geometric parameters, L, h, and H, were varied systematically, as shown in Table 1. The standard geometry was $L = 40$, $h = 300$, and $H = 400$ mm. In all

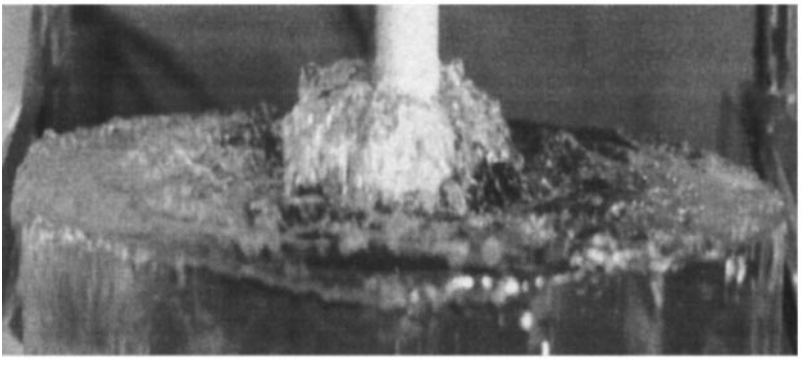

(a)

(b)

Figure 2. Oscillating free surface in swell flapping.

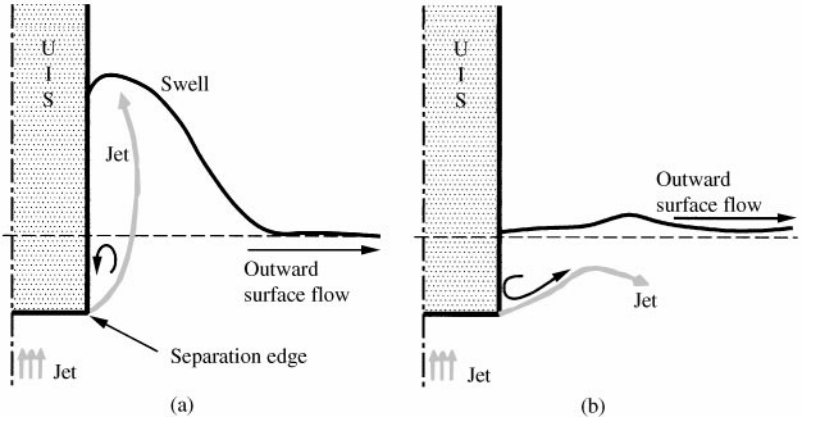

Figure 3. Schematics of jet and swell in swell flapping.

cases, the mean inlet velocity of the jet, V, was varied from 0·47 to 3·78 m/s. Since water was supplied to the test-tank by a head-tank having a constant water level, no pulsation from the pump was imparted to the inlet jet. The entrance length of the inlet channel was more than 500 mm, resulting in a fully developed inlet flow. The Reynolds number at the jet inlet channel was more than 28 000, i.e., a turbulent jet.

The occurrence of oscillation was judged with the naked eye in all experiments. When the height of the fluctuating swell around the UIS was larger than 20 mm, the system was considered to be in oscillation. The water level in the tank was measured by a capacitance-type level meter made from 1·0 mm diameter enamel. It was set at the point of $r = 48$ mm, i.e., 10 mm from the UIS. The oscillation period was calculated using Fast Fourier Transform analysis of the water level fluctuation.

2.2. Results and Discussion

2.2.1. Swell flapping

Under a certain condition of jet velocity, V, and UIS depth, L, a self-induced free-surface oscillation was observed. Figure 2 shows photographs of the oscillating surface. The surface at maximum and minimum amplitude is shown in Figures 2(a) and 2(b), respectively. In the oscillation, the conditions with and without the swell were repeated periodically. Because of the overflow at the cylindrical tank, there was little water-level fluctuation near the tank wall. The free surface oscillated only around the UIS with the swell. The oscillation was completely different from the familiar sloshing in a tank. This oscillation was called "swell flapping".

The flow pattern around the UIS during swell flapping, which was investigated by using a short tuft and ink, is schematically shown in Figure 3. Figures 3(a) and 3(b) correspond to Figures 2(a) and 2(b), respectively. An upward inlet jet impinges on the bottom of the UIS, resulting in a separated flow at the edge of the UIS. The separated jet flutters in synchronism with the axisymmetrical surface swell flapping. The flow has an outward velocity near the free surface. The inlet jet does not fluctuate. The oscillation is thought to be induced by the interaction between the separated jet and the free surface.

2.2.2. Oscillating region

(a) Effects of UIS depth, L

Figure 4 summarizes the onset condition of the swell flapping with the parameters of inlet jet velocity, V, and UIS depth, L. In Group I experiments, the inlet jet velocity, V, and the UIS depth, L, were varied from 0·47 to 3·78 m/s and from 10 to 120 mm, respectively. All other geometrical parameters were fixed at the standard figures. The onset condition of the swell flapping depended on V and L. At a certain L, the swell flapping occurred in a certain velocity range. With increasing UIS depth, swell flapping was observed with a higher inlet jet velocity. On the other hand, swell flapping could not occur over a certain inlet velocity. Over the upper limit of the onset velocity, the separated jet splashed while generating a water curtain. The oscillation could not occur, since the separated jet had little relation with the free surface.

The relation between V and L in the swell flapping was similar to that in the "Jet-Flutter" (Madarame *et al.* 1993), where L corresponded to the distance from inlet to surface or edge, respectively. The swell flapping may have a similar mechanism with the "Jet-Flutter".

(b) Effects of the distance from inlet to surface, h

The swell flapping was related to the separated jet at the UIS. Because the velocity distribution of the inlet jet impinging on the UIS was a function of the distance from the inlet, the separated jet velocity was also a function of the distance from inlet to UIS, $(h - L)$. In the case of Group II experiments, the distance from inlet to surface, h, was adjusted to

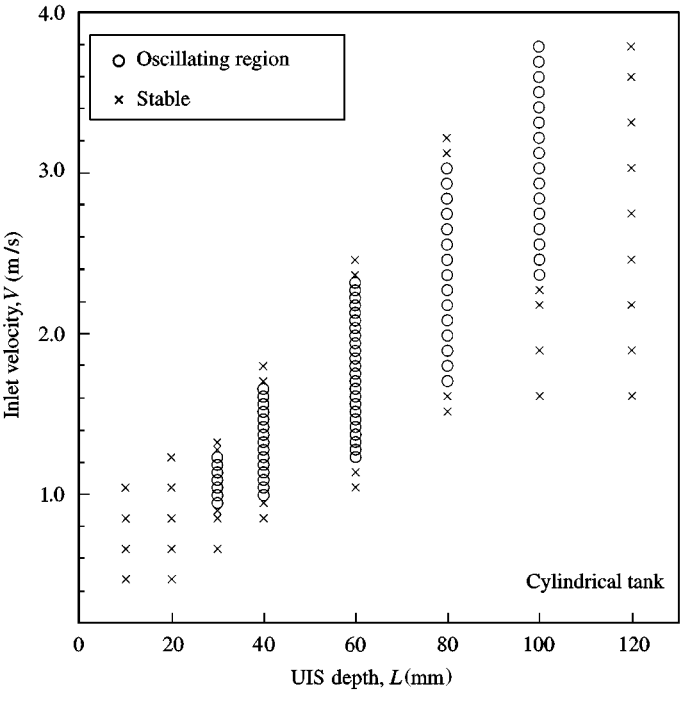

Figure 4. Oscillating region with varying L (Group I experiments: $h = 300$: $H = 400$).

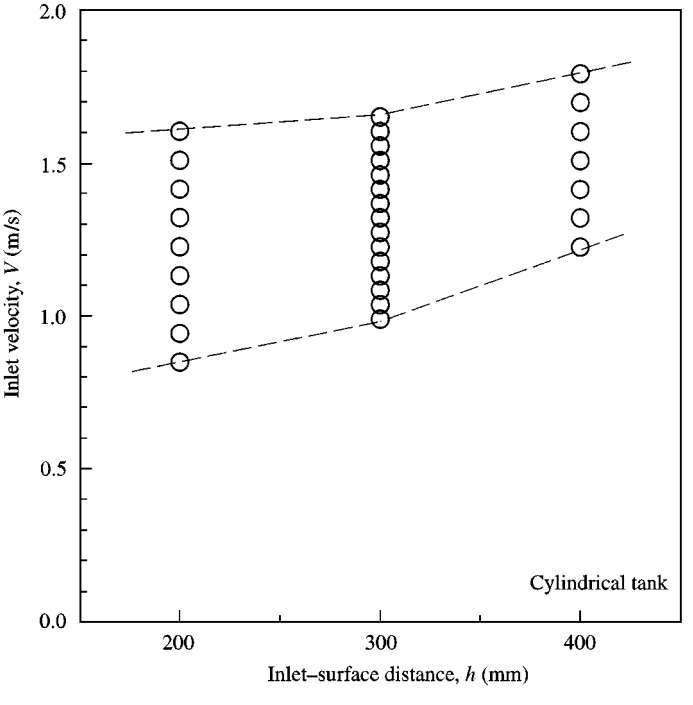

Figure 5. Oscillating region with varying h (Group II experiments: $L = 40$: $H = 400$).

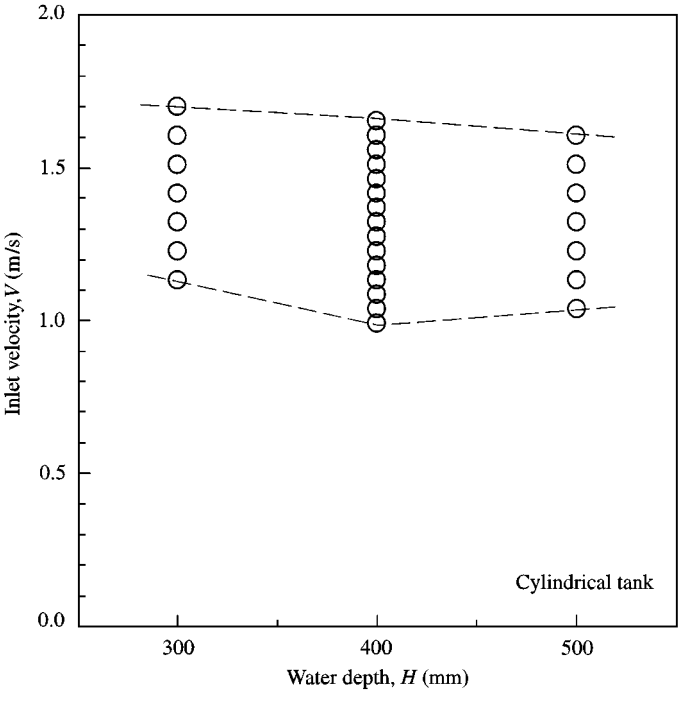

Figure 6. Oscillating region with varying H (Group III experiments: $L = 40$: $h = 300$).

200, 300 and 400 mm, with $L = 40$ mm and $H = 400$ mm constant. Figure 5 shows the onset velocity condition of the swell flapping. With increasing h, the upper and lower limit velocities of the swell flapping increased.

The potential core length of an axisymmetric turbulent free jet is 5–8 times the jet diameter. The potential core length in the experiments was about 340–540 mm, while the jet diameter was 67 mm. The distance from the inlet to the UIS, $(h - L)$, was between 160 and 360 mm. Thus, the jet impinging on the UIS was in the potential core. Although the core velocity in the potential core is constant, the velocity around the potential core diffuses because of the surrounding flow. With increasing h, the separated jet velocity decreases. Therefore, the onset velocity condition of the swell flapping increases with increasing h.

(c) Effects of the water depth, H

Figure 6 shows the onset velocity condition of swell flapping with varying water depth, $H = 300$, 400 and 500 mm (Group III experiments). The water depth had little influence upon the occurrence of swell flapping. This result indicates that swell flapping does not relate to sloshing, since sloshing growth depends on the water depth. In these experiments, the geometric relations among jet, UIS and surface were the same, i.e., with the same separated jet. Therefore, the water depth, H, had little influence on swell flapping.

2.2.3. Oscillation period

(a) Effects of UIS depth, L, and jet inlet velocity, V

The occurrence of swell flapping was governed mainly by jet inlet velocity, V, and UIS depth, L. Figure 7 summarizes the oscillation periods of swell flapping in Group I experiments. The period increases with increasing jet inlet velocity, V, and/or with decreasing UIS

depth, L, while the height of the swell, ξ, increases with increasing period. The oscillating period was thought to relate to the height of the swell, ξ. In "Jet-Flutter" the period relates to the distance from the jet inlet channel to the top of the surface swell, $L + \xi/2$. Also the period of swell flapping may bear a strong relation to the swell height and the separated jet velocity. However, the swell height could not be measured in the cylindrical tank system.

(b) Effects of other geometric parameters, h, H

The effects of the distance from the inlet to the surface, h, and of the water depth, H, on the swell flapping period were investigated. Figure 8 summarizes the oscillation periods with varying jet inlet velocity at a constant $L = 40$ mm. Figure 8 indicates that the water depth, H, did not affect the period of the swell flapping, while the distance from inlet to surface, h, did. The period became longer with decreasing h with a given inlet velocity. The separated jet velocity at UIS decreased with increasing h, causing the swell height to decrease, resulting in a shorter period. The height of the swell was related to the period of swell flapping.

2.3. Summary

Swell flapping was observed in a cylindrical tank with an upward round jet, a free surface, and an upper-inner structure (UIS). The swell flapping was a self-induced free-surface oscillation in which the axisymmetrical surface swell around the UIS oscillated. The characteristics of swell flapping were investigated, and the following were found:

(i) the onset conditions of swell flapping were dependent mainly on the jet inlet velocity, V and UIS depth, L;

(ii) the oscillation period of swell flapping was also dependent on the jet inlet velocity, V and UIS depth, L; the periods were thought to be related to the height of the swell.

3. EXPERIMENTS IN A RECTANGULAR TANK SYSTEM

In the cylindrical tank system, the swell height could not be measured. However, it was thought to be very important for modelling and clarifying the mechanism of "swell flapping". Therefore, the authors carried out additional experiments, now using a rectangular tank system.

3.1. Experimental Apparatus

A cross-sectional view of the experimental apparatus is schematically shown in Figure 9. The rectangular main tank, made of transparent acrylic resin, was 500 mm wide and 100 mm thick. The jet inlet channel 10 mm in width was set at the bottom right.

An upward plane wall jet was injected into the rectangular tank from the inlet channel. The jet impinged on the bottom of an UIS, which had the same cross-section as the inlet jet. The UIS was submerged in the water just above the jet inlet channel. The jet was separated at the edge of the UIS. In this study, the jet separated at the UIS lower edge was called "separated jet". The separated jet impinged on the free surface. The water then overflowed from a left side-weir 150 mm in height. All components of the test-section were stiff enough to not resonate with fluid oscillations.

Here, the possibility of the occurrence of other oscillations is the reason why the plane wall–jet system was selected. Using the plane free jet in the experiments means using the symmetric rectangular system with a cross-section similar to Figure 1. In the symmetric

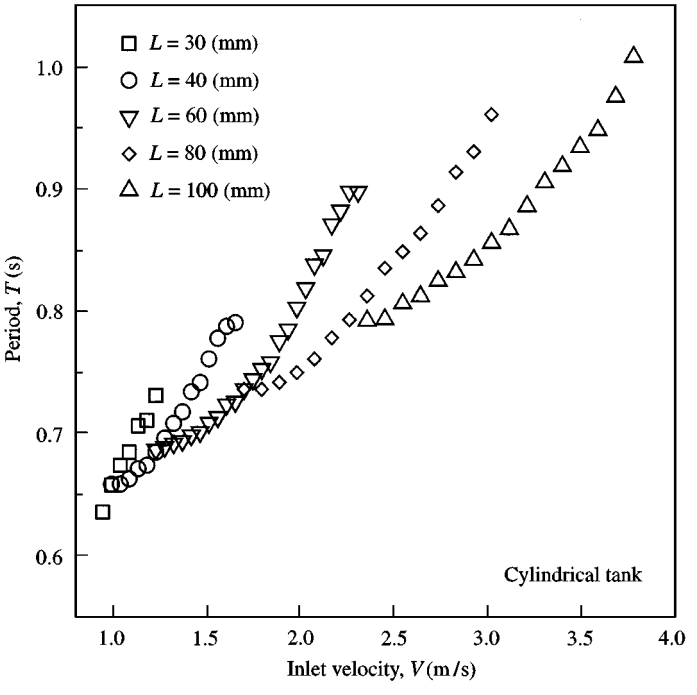

Figure 7. Dependence of frequency on V and L (Group I experiments: $h = 300$: $H = 400$).

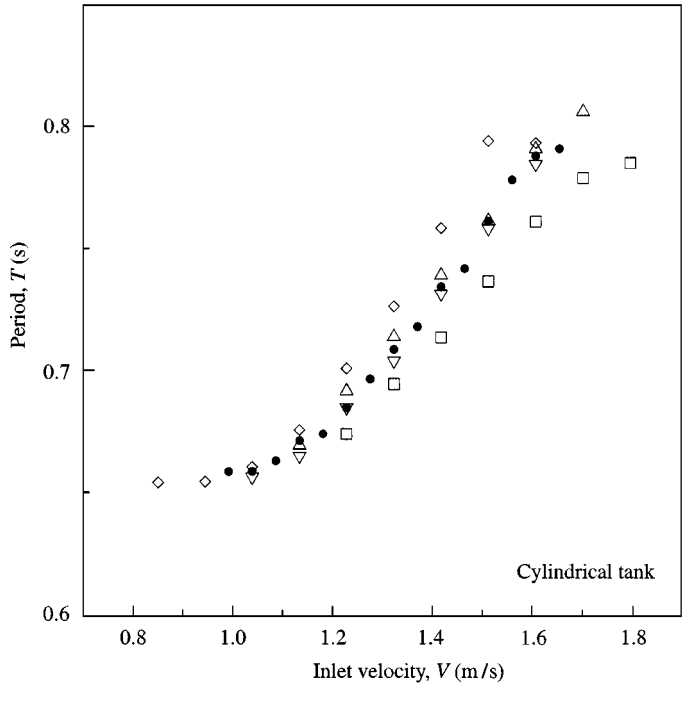

Figure 8. Dependence of frequency on V for $L = 40$ mm: ●, $h = 300$, $H = 400$; ◇, $h = 200$, $H = 400$; □, $h = H = 400$; △, $h = H = 300$; ▽, $h = 300$, $H = 500$, all in mm.

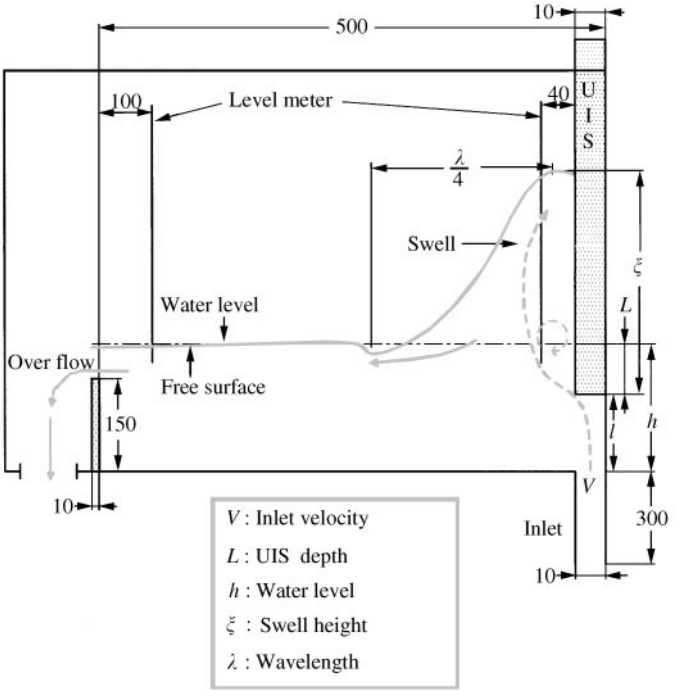

Figure 9. Cross-sectional view of the test tank; dimensional in mm.

rectangular system, the UIS and the jet inlet are set at the centre axis. The injected jet can flow to the right and left side of the UIS. In this case, only the U-tube oscillation due to the "edge-tone" (Powell 1961) was observed. In order to investigate swell flapping, U-tube oscillation and any other fluctuations of the inlet jet before its impingement on the UIS must be avoided; therefore, the wall–jet system was used.

In the experiment, the mean inlet velocity of jet, V, was varied from 0·33 to 3·3 m/s. Since water was supplied to the test-tank by a head tank having a constant water level, no pulsation from the pump was imparted to the inlet jet. The entrance length of the inlet channel was 300 mm, resulting in the inlet flow being fully developed. The Reynolds number in the jet inlet channel was between $6{\cdot}6 \times 10^3$ and $6{\cdot}6 \times 10^4$, i.e., a turbulent jet ($\mathrm{Re} = Vd/v$, V being the jet inlet velocity, d the hydraulic diameter of the jet inlet channel, and v the kinematic viscosity). The distance from inlet to the bottom of the UIS, l, was varied from 20 to 140 mm in 20 mm steps.

The water level in the tank was measured by capacitance type level meters 1·0 mm in diameter. They were set at the points of 40 mm (A) and 400 mm (B) downstream from the UIS. Since the mean water level, h, was a function of V, the relationship between h and V was measured under nonoscillating conditions. The mean water level, h, was defined as the average value of the measured water level at B, near the overflow weir, during 3 min. UIS depth, L, was the difference between h and l. The oscillation period was calculated using fast Fourier transform analysis of water level fluctuations measured at A.

Flow visualization was carried out in order to clarify the jet behaviour. The water in the tank was initially dyed with ink. Additionally, a small quantity of liquid ink was injected upwards along the UIS. The separated jet was then visualized negatively, i.e., the separated jet was not dyed and bright. By analysing the VTR images, the surface shapes and flow pattern were investigated.

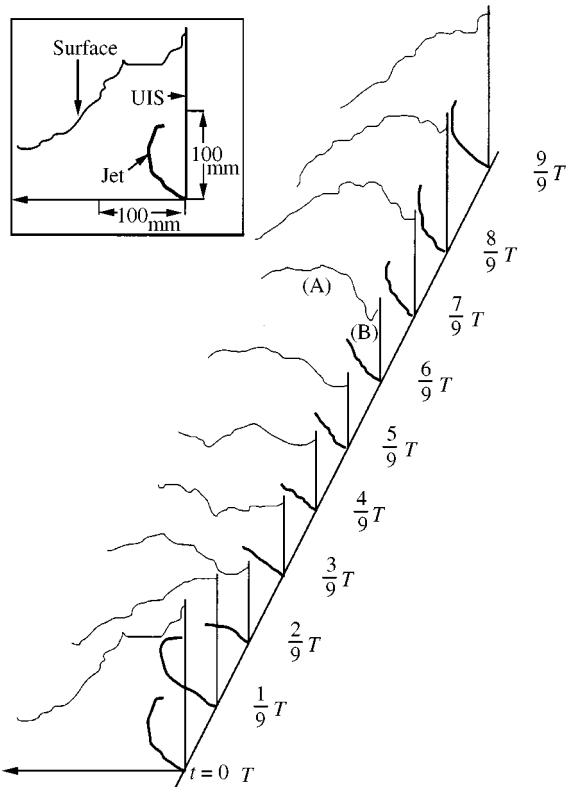

Figure 10. Oscillating free surface and separated jet in swell flapping; $l = 100$ mm, $V = 1{\cdot}33$ m/s, $T = 0{\cdot}95$.

3.2. Results and Discussion

3.2.1. Visualization of surface and jet

Figure 10 shows the surface shapes and the separated jet behaviour during swell flapping under the conditions of $V = 1{\cdot}67$ m/s, $h = 172$ mm, $L = 72$ mm ($l = 100$ mm). In this case, the oscillation period, T, was 0·9 s. Figure 10 resulted from visualized images as shown in Figure 11. Figure 11 shows VTR images at $t = 0$, $\frac{2}{9}T$, $\frac{6}{9}T$, $\frac{8}{9}T$ and $\frac{9}{9}T$ ($\equiv 0T$).

In case of separated flow, the velocity and its gradient is largest not at the centre of the jet, but at the boundary layer between the jet and the separation vortices. Therefore, the streak-line drawn in Figure 10 and the bright line in Figure 11 represent the separation line.

In swell flapping, the separated jet after impingement on the UIS fluttered, and the free surface only around the UIS oscillated. During the oscillation, the conditions with and without the swell were repeated periodically, while the inlet jet did not fluctuate. In the narrow region between the separated jet and the UIS, the separation vortex was observed and the bubbles were rolled up from the free surface. Due to many bubbles and high turbulence, it was impossible to quantitatively estimate details of the separated jet, such as the separation angle of the jet at the bottom edge of the UIS.

The reflection (inward) wave from the left side-weir of the tank generated high turbulence in collision with the progressive (outward) wave. However, the reflection wave could not come up to and affect the oscillating surface around the UIS. Figure 10 shows the surface

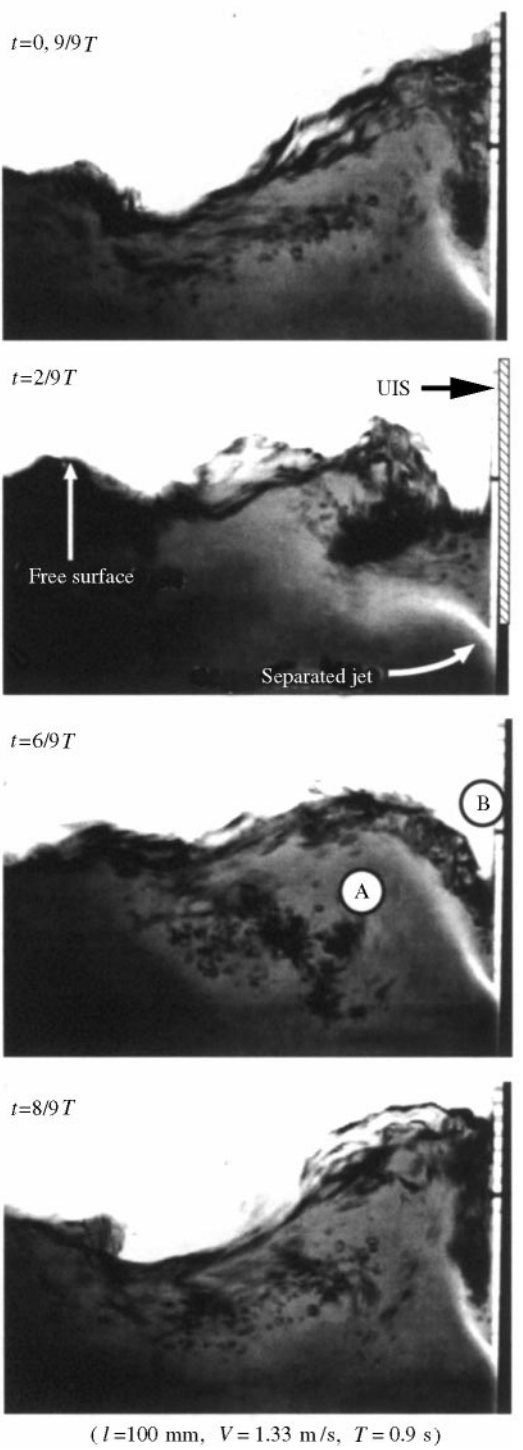

(l=100 mm, V=1.33 m/s, T=0.9 s)

Figure 11. Visualized images of swell flapping.

shapes only near the UIS. The oscillating surface and jet could be considered to be two-dimensional. Hence, we can discuss the surface and jet behaviour during oscillation with the help of Figures 10 and 11.

At $t = 0$ and $\frac{9}{9}T$, the surface swell was the highest. There was a large separation vortex in the narrow region between the free surface and the UIS. The separated jet began to lie down upstream (near the edge of UIS), while it was directed to the UIS (right side) downstream. The surface swell began to break at the next moment, $\frac{1}{9}T$, rolled-up bubbles moved away from the UIS side wall, and the separated jet was bent considerably.

At $\frac{2}{9}T$, the jet lay down almost horizontally. The separation vortex with bubbles flowed away from the UIS side downstream (left side) through the pass between the free surface and the jet. The free surface was flat and smooth at the next moment ($\frac{3}{9}T$) without the separation bubbles, while the separated jet was already directed upward again. From $\frac{2}{9}T$ to $\frac{3}{9}T$, Figure 10 shows that the swell propagates downstream (left side).

A new separation vortex began to be developed and the jet was gradually rising again from $\frac{4}{9}T$ to $\frac{6}{9}T$. The surface at the downstream side (indicated by A in Figure 11), swelled up, while the surface between the jet and the UIS (indicated by B), kept a lower level. Then, the surface (B) started to swell up at $\frac{6}{9}T - \frac{7}{9}T$. At $\frac{8}{9}T$, the jet finished rising vertically, and the surface (B) continued to swell up. At last, $\frac{9}{9}T$, the surface (B) reached the highest point. The separated jet already began to lie down. These processes were then repeated periodically.

Under these conditions, the swell breaking takes about one-third of the period $[(0 \sim \frac{3}{9}T); \frac{1}{3}T]$, while the swell rising takes about two-thirds of the period $[(\frac{3}{9}T \sim \frac{9}{9}9T); \frac{2}{3}T]$. The swell flapping was not a sinusoidal oscillation. The phase of the surface oscillation was delayed from that of the jet fluctuation. In this case, the phase difference was about $\pi/9$.

During swell rising, initially the downstream side surface, surface (A), swelled to the peak height. Then, keeping the level of surface (A), the surface between the jet and the UIS, surface (B), swelled up. Therefore, the swell rising interval could be divided into two: the downstream-side (left side) swell rising term intense and the UIS-side swell rising intense.

3.2.2. Oscillating region

The free surface and the separated jet behaviour were evaluated carefully at various inlet velocities, V, and UIS depths, L (i.e., $h - l$). Figure 12 summarizes the onset conditions of the swell flapping. In these experiments, no hysteresis was observed, showing the reproductivity of the oscillation. Swell flapping was observed under the conditions shown by "o". In some conditions of higher velocity, shown by "◇", large turbulence disturbed the free surface so much that the oscillating period became unstable. As shown in Figure 12, the onset conditions of swell flapping depended on V and L. At a certain L, swell flapping occurred in a certain velocity range. With increasing UIS depth, the lower limit of the jet inlet velocity also increased. As shown in Figures 12 and 4, the characteristics of the onset conditions of swell flapping in the rectangular system were quite similar to those in the cylindrical tank system.

3.2.3. Swell height

In the experiments with the cylindrical tank system, the surface shape could not be measured quantitatively. However, the authors pointed out that the swell height was thought to have a close relation to the swell flapping period. That point was suggested by the fact that the swell height became larger and the oscillating period became longer with increasing jet inlet velocity; this also held true in experiments with the rectangular tank. Besides, in swell flapping in the rectangular tank, only the downstream side surface

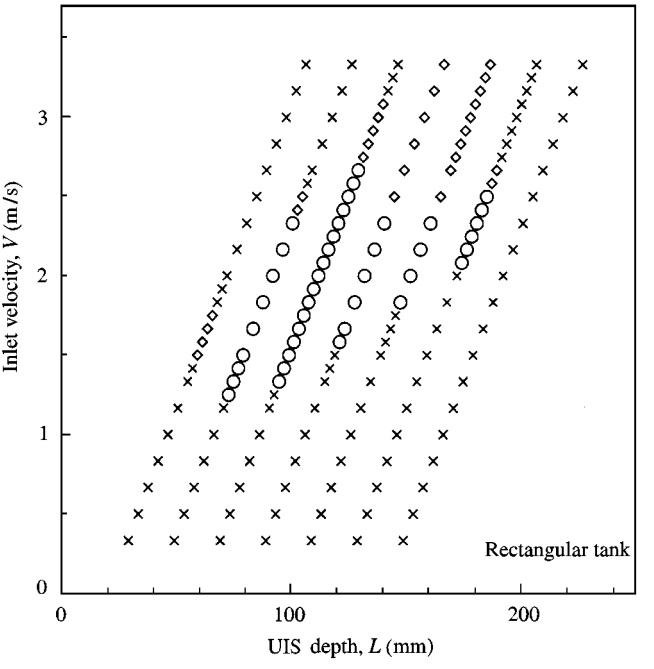

Figure 12. Oscillating region of swell flapping in the rectangular tank: ○, swell flapping was observed; ×, there was no surface oscillation; ◇, the free surface oscillated as swell flapping, but its oscillation period was not constant due to large turbulence.

(indicated by A in Figure 11) swelled up at first, and then, the surface of the UIS side of the separated jet (indicated by B in Figure 11) swelled up while keeping the downstream surface height. Therefore, the importance of the swell height became even larger.

In the experiments with the the rectangular tank, we could measure the maximum swell height from VTR images at every 1/30 s step. Figure 13 summarizes the maximum swell height, ξ, during the oscillation with the inlet velocity, V. In Figure 13, the maximum swell height was the average value of 50 data of 50 periods. The highest points of the surface swell were almost on the UIS wall.

As shown in Figure 13, the swell height, ξ, i.e. the distance from the bottom of the UIS to the maximum point of the swell, depended only on the jet inlet velocity, independently of the UIS position. The swell height, ξ, was proportional to the jet inlet velocity, at least under the present experimental conditions.

3.2.4. Oscillating period

(a) Measured Period

Figure 14 summarizes the oscillating period with the inlet jet velocity. The oscillating period of swell flapping depends only on the jet inlet velocity, independently of the UIS position. The period was expressed as a linear functional formula of the velocity, by applying the least squares technique:

$$T(\mathrm{s}) = 0{\cdot}371V\ (\mathrm{m/s}) + 0{\cdot}350. \tag{1}$$

Figure 14 shows that the oscillation period was prolonged with increasing jet inlet velocity. Figure 10 showed that swell flapping was not a sinusoidal oscillation and the swell rising interval was longer than the swell breaking one.

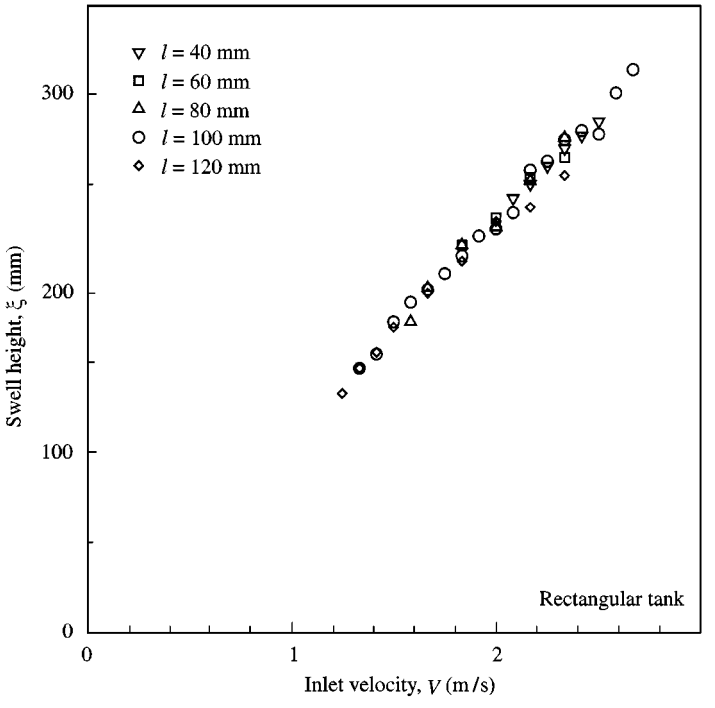

Figure 13. Relation between the inlet velocity and the swell height.

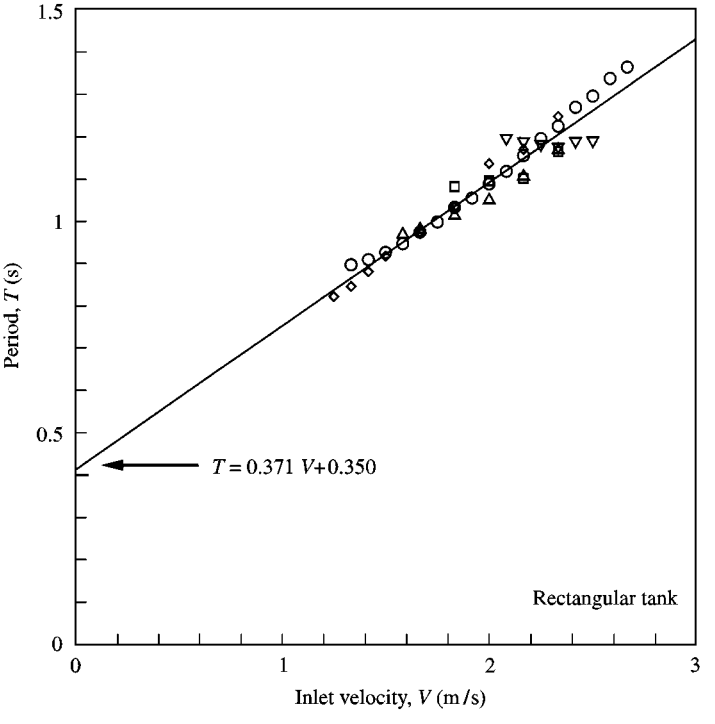

Figure 14. Relation between the inlet velocity and the period: ▽, l = 40 mm; □, l = 60 mm; △, l = 80 mm; ○, l = 100 mm; ◇, l = 120 mm.

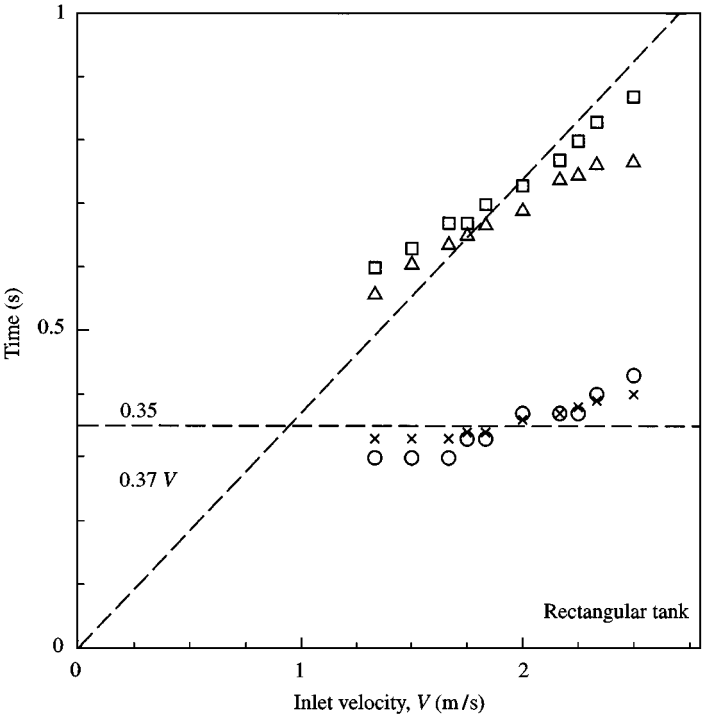

Figure 15. Time for swell rising up and for breaking down: T_{up}(EXP) and T_{down}(EXP) were measured in experiments under various velocity conditions at $l = 100$ mm. T_{up}(CAL) and T_{down}(CAL) were calculated by equations (2) and (3), respectively: □, T_{up}(EXP); ○, T_{down}(EXP); △, T_{up}(CAL); ×, T_{down}(CAL).

Figure 15 shows the swell rising interval (T_{up}(EXP)) and the swell breaking term (T_{down}(EXP)) in the condition of $l = 100$ mm. They were measured by using visualized VTR images at every 1/30 s step. As shown in Figure 15, the first and the second terms of equation (1) represented T_{up}(EXP) and T_{down}(EXP), respectively. In other words, the period of swell rising (T_{up}) increased with increasing jet inlet velocity, V. The swell breaking interval (T_{down}) was almost constant.

(b) Swell rising terms

As shown in Figure 10, the swell rising period was divided into two processes. Initially, the downstream surface (A) swelled to the peak. Keeping the level of surface (A), the surface between the jet and the UIS (B) swelled up, as shown in Figure 16(a). In the actual oscillation, these two processes were closely related. However, in this study, to simplify the model, the interaction between the two processes was neglected.

In the first process, the downstream swell rising period was assumed to be the time intense of the jet free fall. The distance of free fall, ξ, is expressed as $1/2gt^2$. Then, the downstream side swell rising period, T_{up1}, was assumed to be

$$T_{up1} = \sqrt{\frac{2\xi}{g}}. \tag{2}$$

In the second process, the UIS-side swell rising period, the free surface in the narrow region between the separated jet and the UIS moved upward to the maximum point.

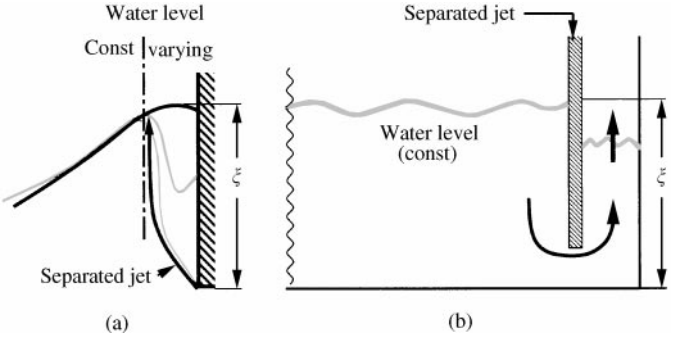

Figure 16. The concept of the model for T_{up2}.

In this study, the UIS side swell rising period was modelled with the analogy of "Jet-flutter" (Madarame, *et al.* 1993). When a jet was injected into a rectangular tank from the bottom center and impinged on the free surface, making a swell, "Jet-flutter" was observed. "Jet-flutter" is the lateral oscillation of the jet synchronized with the surface swell fluctuation. The frequency of Jet- flutter coincided with the natural frequency of the water column oscillation in two equal pillar tanks connected at the distance, h_j, from the surface. Here, h_j was the distance from inlet to surface in the test tank. In Jet-flutter, the jet in the tank, except near the inlet channel, acted as a solid-wall partition.

In the UIS-side swell rising period of swell flapping, a similar behaviour as in Jet-flutter was assumed. The separated jet acted as a solid wall except near the separation point, where the jet played a role of a connector. On the left side of the separated jet, i.e. the downstream side, the water level was constant. Figure 16(b) shows a large tank with a branch pipe, ξ long. The UIS side swell rising period, T_{up2}, was equal to half the period of water column oscillation in the tank shown in Figure 16(b):

$$T_{up2} = \pi\sqrt{\frac{\xi}{g}}. \tag{3}$$

According to the above discussion, the swell rising period, T_{up}(CAL), may be is expressed as

$$T_{up}(\mathrm{CAL}) = T_{up1} + T_{up2} = (\pi + \sqrt{2})\sqrt{\frac{\xi}{g}}, \tag{4}$$

where T_{up1} and T_{up2} are the periods (intervals) for the downstream-side surface swell rising and for the UIS-side surface swell rising, respectively. These surface swell risings were caused by the inlet jet and pressure balance, respectively.

Figure 15 also shows the calculated results, using the measured swell height, ξ. As shown in Figure 15, the calculated term, T_{up}(CAL), roughly correspond to the experimental, T_{up}(EXP). Under high velocity conditions, the discrepancy was caused by the turbulent surface.

(c) Swell breaking terms

As shown in Figure 15, the swell breaking period, T_{down}(EXP), represented by open circles, was almost constant, independent of the jet inlet velocity and/or the maximum swell height. The swell was propagated from upstream to downstream as shown in Figure 10, in $2/9T$. Wave propagation did not depend on the inlet velocity. Though the swell height was large, a shallow-water wave was assumed in order to linearize things. Considering the swell

breaking term as half of the wave propagation period, T_{down}(CAL) was expressed as

$$T_{down}(\mathrm{CAL}) = \frac{1}{2}\lambda\sqrt{\frac{g\lambda}{2\pi}\tanh\frac{2\pi h}{\lambda}}, \tag{5}$$

where λ is the wavelength. In this study, the wavelength was defined from the wave shape as shown in Figure 9. In Figure 15, T_{down}(CAL) was calculated by equation (5). T_{down}(CAL) agreed well with T_{down}(EXP). In Figure 15, both T_{down}(EXP) and T_{down}(CAL) increase a little with increasing inlet velocity. With increasing inlet velocity, the wavelength also increased, resulting in an increase of T_{down}(CAL) according to equation (5).

4. CONCLUSION

Swell flapping, a newly discovered self-induced free-surface oscillation, was observed in both a cylindrical and a rectangular tank system with a jet, a free surface and a structure. With the cylindrical tank system, the onset conditions and the oscillation period were investigated with changing geometric parameters. It was pointed out that the swell height during oscillation might have an important correlation with the oscillating period. Therefore, with the rectangular tank system, the swell height and the period of oscillation were experimentally investigated with visualization studies. The period of swell flapping was modelled simply with the swell height. The following conclusions were arrived at.

(a) Swell flapping could occur at a certain jet inlet velocity and UIS depth.

(b) The maximum swell height during the oscillation was proportional to the jet inlet velocity, independently of the UIS depth.

(c) The swell flapping period could be divided into two: the swell breaking period and the swell rising period.

(d) The oscillation period of swell flapping was expressed as a linear functional of the jet inlet velocity. The swell rising period was proportional to the jet inlet velocity. The swell breaking period was almost constant.

(e) The swell rising period could itself be also divided into two. Initially, only the downstream-side surface of the separated jet swelled. Then, the surface between the jet and the UIS swelled up, keeping the downside surface level.

(f) The downward swell rising period was assumed to correspond to that of the jet free fall. The UIS-side swell rising period was assumed to be equal to the half-period of water column oscillation.

(g) The swell breaking period closely agreed with the wave propagation period.

APPENDIX : NOMENCLATURE

g	gravitational acceleration (m/s^2)
H	mean water depth (mm)
h	distance from jet inlet channel to UIS (mm)
L	UIS depth (mm)
T	oscillation period (s)
T_{up}	swell rising interval (s)
T_{down}	swell breaking interval (s)
V	mean jet inlet velocity (m/s)
λ	wavelength of surface swell (mm)
ξ	maximum swell height (mm)

References

Inagaki, T., Umeoka, T., Fujita, K., Nakamura, T., Shiraishi, T., Kiyokawa, T. & Sugiyama, Y. 1987 Flow induced vibration of inverted U-shaped piping containing flowing fluid of top entry system for LMFBR. *Transactions of International Conference on Structural Mechanics in Reactor Technology*, **9-E**, pp. 295–302.

Hara, F. 1990 Experimental study on sloshing characteristics of a flowing liquid in a Tank. *JSME International Journal*, Series III, **33**, 330–338.

Fukaya, M., Madarame, H., Okamoto, K., Iida, M. & Someya, S. 1995 Self-induced free surface oscillations caused by water jet. *JSME&ASME 3rd International Conference on Nuclear Engineering*, Vol. **1**, pp. 595–602.

Madarame, H., Iida, M., Okamoto, K. & Fukaya, M. 1993 Jet-flutter: self-induced oscillation of upward plane jet impinging on the free surface. *Proceedings of the Asia Pacific Vibration Conference '93*, Vol. **1**, pp. 265–270.

Powell, A. 1961 On the edgetone. *Journal of the Acoustical Society of America* **33**, 395–409.